https://doi.org/10.33271/nvngu/2021-5/022

A. P. Akinola[1],
orcid.org/0000-0002-4706-2124,
T. B. Afeni[2],
orcid.org/0000-0001-8216-8007,
R. A. Osemenam[2],
orcid.org/0000-0002-6808-6141

1 – Department of Mining Engineering, University of Jos, Jos, Nigeria, e-mail: akinolaa@unijos.edu.ng
2 – Department of Mining Engineering, Federal University of Technology Akure, Akure, Nigeria

SURFACE MODELLING BY GEOID DETERMINATION FOR FLOOD CONTROL OF EWEKORO LIMESTONE DEPOSIT (NIGERIA)

Purpose. To determine the geoid heights from various control points of the quarry located in the northern and southern zones of the limestone deposit of the Lafarge WAPCO Cement Ewekoro in Ogun State, Nigeria.

Methodology. The GPS and levelling data were used to determine the geoid heights from various control points of the quarry located in the northern and southern zones of the limestone deposit. The geoid heights obtained from GPS-Levelling data were used for three surface models which are polynomial regression model, inverse distance model and nearest neighbour model. These models were used to crossvalidate the geoid heights for the control points.

Findings. The result shows that the deviations of the geoid heights for the GPS/Levelling and models are between 0.03 and 0.01 m respectively. The models were used to generate contour maps that reveal the better location where the flood can be channelled.

Originality. The results can be compared to the data obtainable during operations carried out in the quarry.

Practical value. The flood in the quarry face will be better controlled by creating a sump at the lowest point on the elevation maps and controlled drilling to give better aeration.

Keywords: *Limestone deposit, GPS-levelling, geoid height, surface models, flood control*

Introduction. The management of flood related issues in quarries is one of the most critical problems encountered during mineral exploitation especially in cases of incessant precipitation. An ineffective management could result in suspension of mining activities and even long term abandonment of the quarry in devastating situations. In 2007, Ewekoro quarry suffered disruption of operation as a result of flooding due to the location of the deposit and this reduced the supply of raw material to the production factory.

The distribution of mine flooding is influenced by one global factor. It is the relationship of the ore body to the surface topography. This relationship expresses itself in several ways. The primary influence is on the location and direction of mining [1]. In order to mine from any mining sites with due respect to the natural occurrence like flood, then the topography of the site must be taken so that water would freely drain from the mines.

The expanding uses of geodetic control in support of spatial information systems demand the adoption of reliable procedures to support geo-referencing of spatial data and Geographical Information System (GIS) activities. Therefore, the continuing evolution of Global Positioning System (GPS) and Geographical Information System (GIS) hardware and software as well necessitates the adoption of standards and specification in planning, surveying, methodologies, and implementation of both systems. The links between GIS software and the spatial data produced by GPS or levelling techniques develop the geo-referencing process and the specifications adopted to ensure the given level of the accuracy [2]. A number of factors have led to an increasing need for geo-referencing and spatial data products on a common reference frame that extends across the whole globe. These factors include growing reliance on satellite positioning systems and development of satellite based mapping systems in order to achieve higher resolution [3].

In order to produce or update spatial data related to surveying applications, a network of control points is necessary. Such a network consists of a number of points spread across the area under consideration. By referencing spatial data to such network, the resulting data and information from multiple local surveying activities can be accurately connected [4].

The impact of the GPS is undeniable. In the span of just a few years GPS has become the leading positioning technology [5]. This revolution has not been confined to surveying community, but has extended into mapping, navigation, and GIS applications. Many of these applications require accurate vertical positioning. Generally, coordinates determination from GPS measurements uses the known positions of satellites and the measured distance between satellites and the known points. It is commonly considered as a three-dimensional system (Latitude, Longitude, and ellipsoidal height). But, the heights obtained from GPS are typically heights above an ellipsoid model of the earth [6]. It is a geodetic height which is purely geometrical quantity, and represents the length of the normal to the reference ellipsoid between the ellipsoid and the point of interest. These GPS ellipsoidal heights are not consistence with levelled heights above mean sea level (MSL), often known as orthometric height [7]. The orthometric height is defined as the length of the plumb-line (a line that is always normal to the equipotential surface of the gravity field) between the geoid and the point of interest and as such is intimately related to the gravity field of the earth (Weikko and

Helmut, 1967). Thus, the knowledge of the geoid is necessary for transforming the geodetic to orthometric heights and vice versa. The geoid and ellipsoid intersect at the geoid undulations. Undulations result from several phenomena, the most significant of which is the existence of gravitational anomalies caused by the non-homogeneous nature of the earth.

Reigber, et al. [8] concludes that since its inception in the early 1970s, GPS has become a widely used surveying tool. Today, accuracies at the centimetre level or better are routinely achieved using a variety of relative positioning techniques. These techniques range from near-instantaneous positioning over relatively short reference receiver to unknown receiver distances, to solutions requiring many hours of data and advanced modelling for distances between receivers of up to several thousand kilometres. Removal of the line-of-sight dependency for survey observation has radically altered the practices of the survey community, allowing larger areas and more points to be measured as emphasized by Akeju and Afeni [9].

Relatively, GPS also helps in deformation monitoring and it has been widely used for a number of monitoring applications. Nowadays, regional GPS surveys are used for measurement of plate tectonic motions and to characterize the kinematics and geodynamics of active lithospheric areas for earthquake and volcano hazards [10]. In small-scale deformation monitoring applications, GPS is now used to observe structures which, in the past, may have been monitored using traditional surveying techniques or using inclinometers or extensometers. Examples of successful small scale monitoring using GPS can be found for bridges [11], buildings [12], volcanoes [13], local and regional ground movements due to seismic events [14], and ground subsidence [15].

The geoid height (or geoid undulation) can be defined as the separation of the reference ellipsoid with the geoid surface measured along the ellipsoidal normal. The classical Gauss-Listing definition of the geoid is given as an equipotential surface of the Earth's gravity field that coincides with the mean sea level [16]. Today, it is well known that this is not a strictly correct definition as MSL departs from the equipotential surface by up to two meters due to various oceanographic phenomena, such as variable temperature, salinity, instantaneous sea surface topography, and so on [16].

Ellipsoidal heights obtained with GPS do not reflect the natural situation. So, they cannot meet precision of practical needs related to heights. However, orthometric heights are more compatible with physical event and so, they are used successfully in solving many problems related to heights in practice. But obtaining orthometric heights with traditional measurements (using levelling instrument) is a very difficult process. Therefore, ellipsoidal heights obtained with GPS easily must be converted to orthometric heights. For this conversion, geoid heights with certain accuracy must be known.

In order to convert the high-precision ellipsoidal heights to orthometric heights, as is required for engineering purposes, the determination of the geoid is necessary. Because the relation between ellipsoidal and orthometric heights involves the geoid undulation [17]. When accurate heights are achieved, then the data can be used to design flood control and reserve estimation.

This research was carried out to design a better way of control flood in a surface mine environment.

Study area. The study area belongs to Lafarge cement WAPCO Nigeria Plc, which is a subsidiary Lafarge Company with their presence in over 64 countries. The cement company formerly bear the name WAPCO Plc but was changed to Lafarge Cement WAPCO Nigeria Plc in 2008 after the Lafarge Company acquired it. Lafarge WAPCO has three plants in Nigeria, one in Shagamu and two in Ewekoro with current production capacity of 4.5 million metric tons per year.

The study area lies within Ogun State, which is bounded in the west by the Benin Republic, in the south by Lagos State, in the north by Oyo and Osun States, and in the east by Ondo State. It occupies a total area of 16 400 km^2. Ewekoro is the host to Lafarge West African Portland Cement quarry and lies between longitude 3° 05′ to 3° 15′E and latitudes 6° 40′ to 6° 55′N.

Overlying the Abeokuta Group conformably is the Imo Group, which is comprised of shale, limestone and marls. The two-lithostratigraphic units under this group are Ewekoro Formation and Akinbo Formation. Adegoke (1977) described the formation as consisting of shaly limestone and about 12.4 m thick which tends to be sandy and divided into three microfacies. This was further modified and fourth unit was proposed. It is Paleocene in age and is associated with shallow marine environment due to abundance of coralline algae, gastropods, pelecypods, echinoid fragments and other skeletal debris. Akinbo Formation lies on the Ewekoro Formation and it is comprised of shale, glauconitic rock bank, and gritty sand to pure grey and with little clay. Lenses of limestone deposit from Ewekoro Formation grades literally into the Akinbo shale very close to the base. The base is characterized by the presence of a glauconitic rock. The age of the formation is Paleocene to Eocene.

Overlying the Imo Group is the Oshosun Formation – sequence of mostly pale greenish-grey laminated phosphatic marls, light grey white-purple clay with interbeds of sandstone. It also consists of claystone underlain by argillaceous Formation. Eocene age is assigned to this formation (Agagu, 1985). The sedimentation of Oshosun formation was followed by a regression, which deposited the limestone unit of Ilaro Formation (Kogbe, 1976). The sequence represents mainly coarse sandy esturine deltaic and continental beds, which show rapid lateral facies change.

The coastal plain sands are the youngest sedimentary unit in the eastern Dahomey basin, it probably overlay the Ilaro Formation unconformably, but convincing evidence as to this is lacking and it consists of soft, poorly sorted clayey sand and pebbly sands. The age is from Oligocene to Recent (Jones and Hockey, 1964).

The study area is located in the sedimentary area of southwestern Nigeria. Ewekoro formation belongs to tertiary-formed Palaeocene and Eocene; and the greater part of the depression is a potential artesian basin where ground water can be sourced. Adegoke, et al. (1976) outlined the Albran and younger Palaeographic history of Nigeria and summarized the nature and extent of transgressive, regressive phases as well as the nature of the sediment. The geology of Ogun State comprises sedimentary and basement complex rocks, which underlie the remaining surface area of the state. It also consists of intercalations of argillaceous sediment. The rock is soft and friable but in some places cement by ferruginous and siliceous materials. The sedimentary rock of Ogun State consists of Abeokuta formation lying directly above the basement complex (Fig. 1). Ewekoro, Oshosun and Ilaro formations in turn overlie this, which are all overlain by the coastal plain sands (Benin formation).

Method. The data available for this study consisted of 100 control points of the GPS readings. The study location was divided into two zones namely (northern and southern zones) based on geologic and lithological arrangement of the deposit and the location of the quarry faces within the deposit and these data were collected from each of the quarries that were located in these two zones.

Determination of the geoid levelling. The samples collected from the field are both GPS coordinates of the quarry bench and the levelling coordinates of the same respective area. The heights from these two methods were used to calculate the geoid of the area using the formula

$$N = h - H,$$

where N is the geoid height; h is the ellipsoidal height; H is the orthometric height.

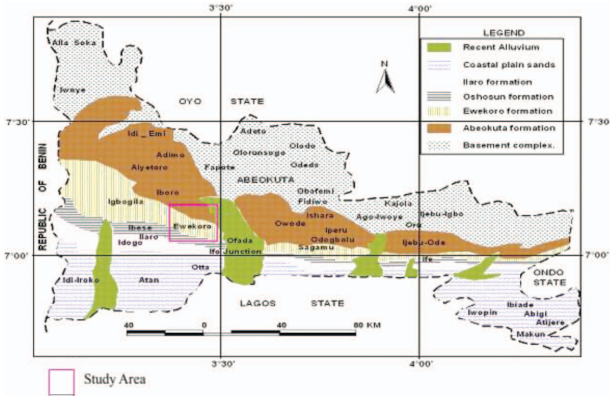

Fig. 1. Geological map of the study area

Determination of geoid heights of test points in different geoid models. Geoid undulation values of 100 selected test points were calculated in Polynomial Regression, Nearest Neighbour and Inverse Distance global geoid models. To obtain the geoid heights firstly, the height anomaly values of points were interpolated according to each model with the program harmp.exe of GOLDEN software (Surfer 9) package by using the known latitude, longitude and heights of points. After that, having applied the correction to the determined height anomalies, geoid heights (N) were calculated. N geoid heights were determined according to the different specified models.

Results. ***Statistical Analysis.*** The geoid heights are calculated from the differences in the ellipsoidal and orthometric heights for the two zones. The adjusted readings are presented in Table 1. The post-maps of the GPS reading for the northern and southern zone of the quarry surface are presented below

Table 2 gives the abridge result of the calculation from the polynomial regression, inverse distance and the nearest neighbour model as used in this work. The result covered 100 control points for both the northern and the southern zones area under consideration. Tables 3–7 and 8 show the statistical analysis of the models as distributed in dispersion.

Comparison of the surface models. Tables 9–13 and 14 show the comparison of the differences in the GPS/Levelling geoid and the geoid from the other models. The Range, Minimum, Maximum, Mean and Standard Deviation of these differences are shown as well.

Surface images generated from the models. Fig. 3 shows the images of the contour maps obtained from the Inverse Distance Model while Fig. 4 shows that obtained from the Polynomial model and Fig. 5 shows that obtained from the Nearest Neighbour Model. Each model figures are presented in three maps that represent the contour maps according to the point of references 25, 50 and 100 for the Northern Zone in that order. Also Figs. 6, 7 and 8 show the contour maps obtained from the Inverse Distance Model, Polynomial regression

Table 1

Geoid heights from the GPS/Levelling (Abridged)

Northern Zone					Southern Zone				
EAST	NORTH	Ellipsoidal Height	Orthometric Height	Geoid (N)	EAST	NORTH	Ellipsoidal Height	Orthometric Height	Geoid (N)
520306.89	764592.50	24.57	23.67	0.90	520643.9	765324.3	24.4	23.4	0.98
520312.87	764596.13	24.54	23.61	0.93	520652.9	765332.9	24.6	24.5	0.12
520316.49	764596.65	24.57	24.38	0.19	520653.5	765315.6	24.3	23.4	0.88
520319.06	764604.68	24.79	24.56	0.23	520658	765337.5	24.6	24.4	0.23
520322.67	764605.16	24.76	24.00	0.76	520663.1	765330.2	24.4	24.3	0.11
520330.38	764613.98	24.76	24.16	0.60	520663.8	765312.5	24.1	23.7	0.33
520334.45	764621.88	24.63	24.17	0.46	520667.6	765345.8	24.8	24.3	0.43
520338.72	764621.90	24.52	24.01	0.51	520668.3	765330.2	24.4	23.9	0.52
520340.35	764621.28	24.78	24.44	0.34	520668.9	765312.6	24.2	23.3	0.83
520343.55	764625.69	24.88	24.04	0.84	520673.6	765321.3	24.0	23.0	1.01

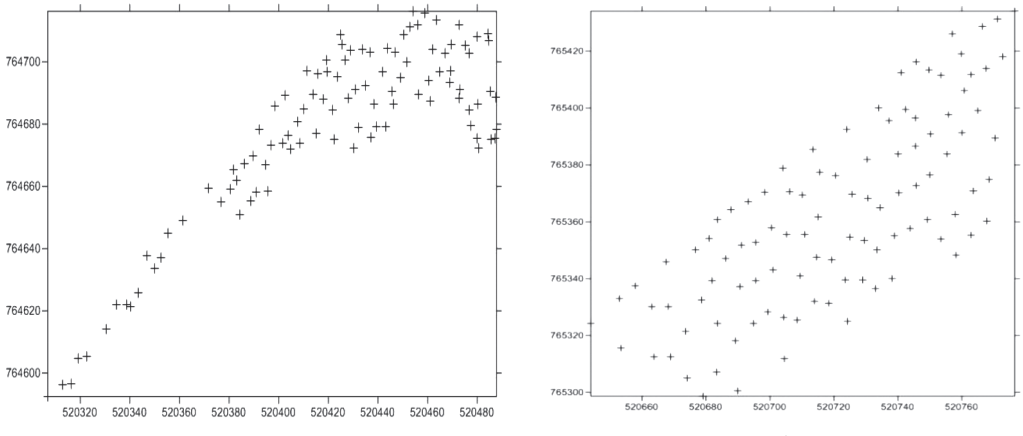

a *b*

Fig. 2. Post map for GPS reading:

a – in the northern quarry face; b – in the southern quarry surface

Table 2

Geoid heights from all the models. (Abridged)

Northern Zone				Southern Zone			
Geoid (*N*)	Polynomial	Inverse	Nearest	Geoid (*N*)	Polynomial	Inverse	Nearest
0.90	0.88	0.89	0.89	0.98	0.99	0.985	0.97
0.93	0.88	0.91	0.91	0.12	0.1	0.11	0.095
0.19	0.12	0.16	0.16	0.88	0.73	0.805	0.79
0.23	0.20	0.22	0.22	0.23	0.31	0.27	0.255
0.76	0.70	0.73	0.73	0.11	0.13	0.12	0.12
0.60	0.55	0.58	0.58	0.33	0.29	0.31	0.295
0.46	0.44	0.45	0.45	0.43	0.43	0.43	0.415
0.51	0.50	0.51	0.51	0.52	0.47	0.495	0.48
0.34	0.33	0.34	0.34	0.83	1.18	1.005	0.99
0.84	0.78	0.81	0.81	1.01	0.91	0.96	0.945

Table 3

Statistical result of the Models from 25 control points (Southern Zone)

Method	Range	Minimum	Maximum	Mean	Std. Deviation
Geoid/Levelling	1.12	0.1	1.22	0.610385	0.36364247
Polynomial Model	1.08	0.1	1.18	0.592308	0.335264763
Inverse Model	1.06	0.12	1.18	0.603077	0.331019869
Nearest Neighbour Model	1.04	0.12	1.16	0.589615	0.329429577

Table 4

Statistical result of the Models from 50 control points (Southern Zone)

Method	Range	Minimum	Maximum	Mean	Std. Deviation
Geoid/Levelling	1.19	0.09	1.28	0.601961	0.342064436
Polynomial Model	1.1	0.1	1.2	0.53451	0.322981818
Inverse Model	1.15	0.09	1.24	0.569608	0.309231051
Nearest Neighbour Model	1.15	0.08	1.23	0.555686	0.308540143

Table 5

Statistical result of the Models from 100 control points (Southern Zone)

Method	Range	Minimum	Maximum	Mean	Std. Deviation
Geoid/Levelling	1.19	0.09	1.28	0.579604	0.308525269
Polynomial Model	1.1	0.1	1.2	0.530297	0.295179455
Inverse Model	1.15	0.09	1.24	0.555941	0.271175877
Nearest Neighbour Model	1.15	0.08	1.23	0.541881	0.270753441

Table 6

Statistical result of the Models from 25 control points (Northern Zone)

Method	Range	Minimum	Maximum	Mean	Std. Deviation
Geoid/Levelling	1.09	0.12	1.21	0.589231	0.364262796
Polynomial Model	1.08	0.09	1.17	0.551538	0.350390551
Inverse Model	1.08	0.11	1.19	0.571154	0.357304653
Nearest Neighbour Model	1.08	0.11	1.19	0.571154	0.357304653

Table 7

Statistical result of the Models from 50 control points (Northern Zone)

Method	Range	Minimum	Maximum	Mean	Std. Deviation
Geoid/Levelling	1.09	0.12	1.21	0.618039	0.318816685
Polynomial Model	1.08	0.09	1.17	0.585098	0.311617538
Inverse Model	1.08	0.11	1.19	0.602353	0.31496405
Nearest Neighbour Model	1.08	0.11	1.19	0.602353	0.31496405

Table 8

Statistical result of the Models from 100 control points (Northern Zone)

Method	Range	Minimum	Maximum	Mean	Std. Deviation
Geoid/Levelling	1.26	0.1	1.36	0.650294	0.324004816
Polynomial Model	1.24	0.09	1.33	0.618922	0.316377725
Inverse Model	1.22	0.1	1.32	0.635784	0.320304423
Nearest Neighbour Model	1.22	0.1	1.32	0.635784	0.320304423

Table 9

Comparison of models by using geoid from 25 control points (Southern Zone)

	Range	Minimum	Maximum	Mean	Std. Deviation
GPS/Lev – Polynomial Model	1.19	–0.6	0.59	0.018077	0.229416987
GPS/Lev – Inverse Model	0.6	–0.3	0.3	0.008846	0.115804211
GPS/Lev – Nearest Model	0.59	–0.28	0.31	0.024615	0.115038455

Table 10

Comparison of models by using geoid from 50 control points (Southern Zone)

	Range	Minimum	Maximum	Mean	Std. Deviation
GPS/Lev – Polynomial Model	1.44	–0.6	0.84	0.067451	0.247385069
GPS/Lev – Inverse Model	0.72	–0.3	0.42	0.033725	0.124803218
GPS/Lev – Nearest Model	0.72	–0.28	0.44	0.049216	0.124158659

Table 11

Comparison of models by using geoid from 100 control points (Southern Zone)

	Range	Minimum	Maximum	Mean	Std. Deviation
GPS/Lev – Polynomial Model	1.82	–0.98	0.84	0.049307	0.266147543
GPS/Lev – Inverse Model	0.91	–0.49	0.42	0.024158	0.133934815
GPS/Lev – Nearest Model	0.91	–0.47	0.44	0.040495	0.133404469

Table 12

Comparison of models by using geoid from 25 control points (Northern Zone)

	Range	Minimum	Maximum	Mean	Std. Deviation
GPS/Lev – Polynomial Model	0.2	–0.07	0.13	0.037692	0.039729857
GPS/Lev – Inverse Model	0.1	–0.03	0.07	0.018846	0.020460092
GPS/Lev – Nearest Model	0.1	–0.03	0.07	0.018846	0.020460092

Table 13

Comparison of models by using geoid from 50 control points (Northern Zone)

	Range	Minimum	Maximum	Mean	Std. Deviation
GPS/Lev – Polynomial Model	0.2	–0.07	0.13	0.032941	0.039914615
GPS/Lev – Inverse Model	0.11	–0.04	0.07	0.016275	0.020587451
GPS/Lev – Nearest Model	0.11	–0.04	0.07	0.016275	0.020587451

Table 14

Comparison of models by using geoid from 100 control points (Northern Zone)

	Range	Minimum	Maximum	Mean	Std. Deviation
GPS/Lev – Polynomial Model	0.23	–0.07	0.16	0.031373	0.037733805
GPS/Lev – Inverse Model	0.12	–0.04	0.08	0.015882	0.019414853
GPS/Lev – Nearest Model	0.12	–0.04	0.08	0.015882	0.019414853

Model and Nearest Neighbour Model for the Southern Zone. Figs. 9 and 10 show the contour maps with elevations of geoid obtained from the Inverse Distance and Nearest Neighbour Model from both the Northern and Southern zones.

Flood control. From Figs. 9 and 10, which are obtained from the Inverse Distance and Nearest Neighbour Models, the quarry face can be prevented from flooding by channelling the sump for each quarry face at the base area of the map (labelled part **A**). The Ewekoro quarry whose operation has reached the second bench and still progressing downward is prone to flooding during the raining seasons, which can bring about halt to the quarry operation and this in turn can hinder the cement production operation. From the elevation plot of the readings from the quarry pit the flood prone areas could be discovered for adequate measures and preventions.

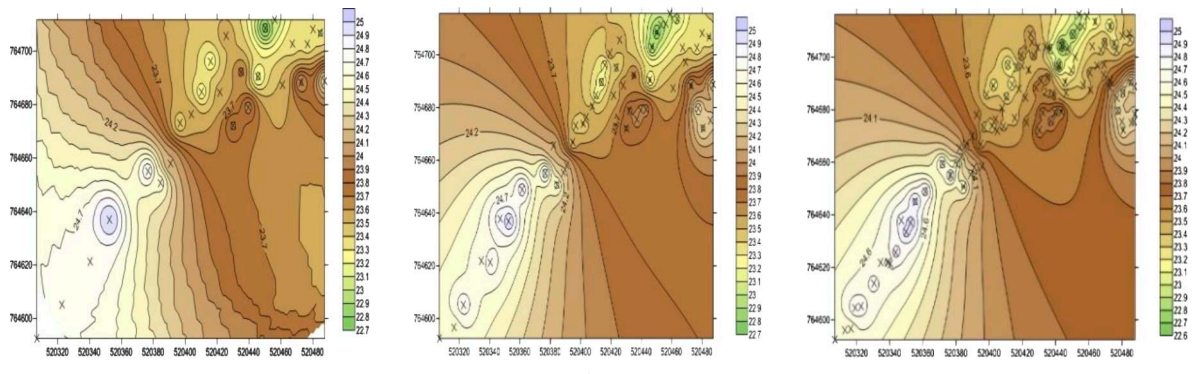

a *b* *c*

Fig. 3. Contour maps of geoid obtained from the Inverse Distance Model (*Northern Zone*):
a – 25 – control points; b – 50 – control points; c – 100 – control points

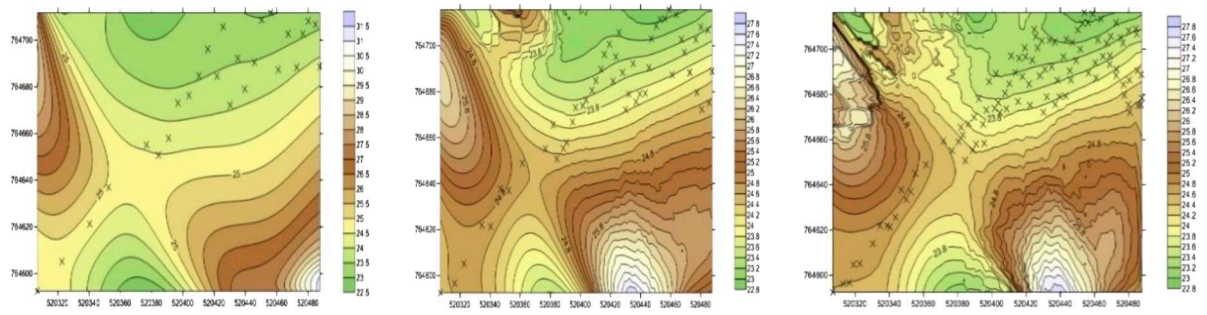

a *b* *c*

Fig. 4. Contour maps of geoid obtained from the Polynomial Regression Model (*Northern Zone*):
a – 25 – control points; b – 50 – control points; c – 100 – control points

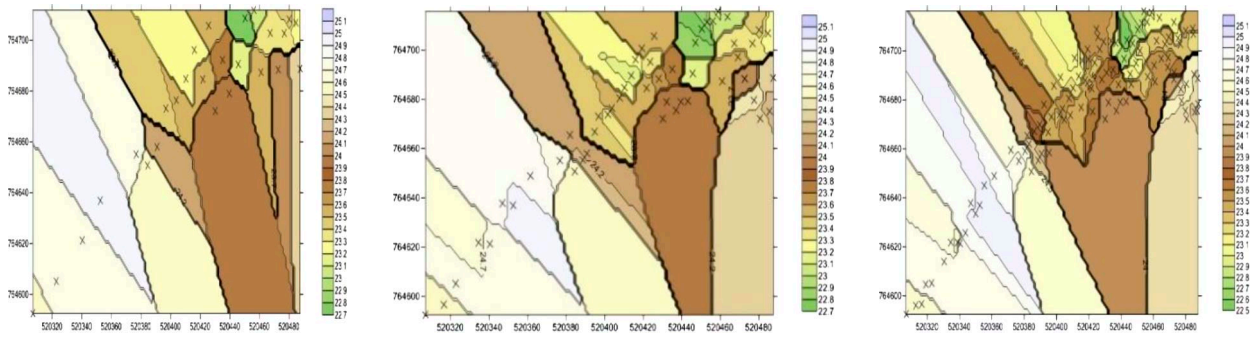

a *b* *c*

Fig. 5. Contour maps of geoid obtained from the Nearest Neighbour Model (*Northern Zone*):
a – 25 – control points; b – 50 – control points; c – 100 – control points

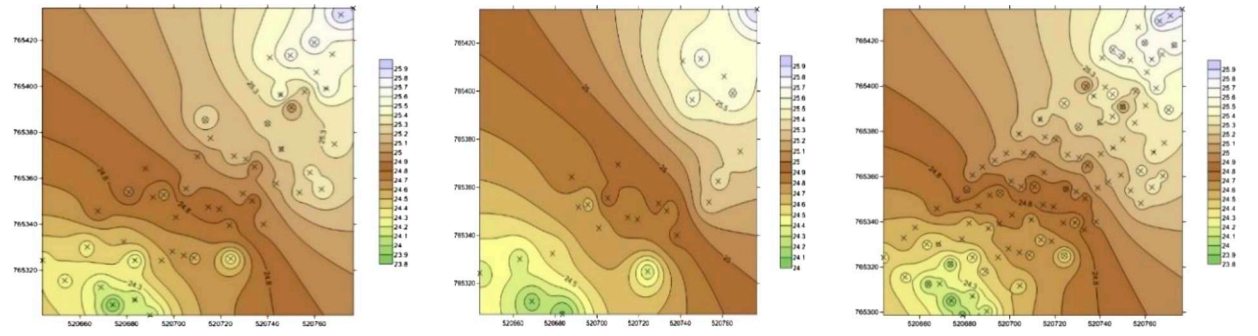

a *b* *c*

Fig. 6. Contour maps of geoid obtained from the Inverse Distance Model (*Southern Zone*):
a – 25 – control points; b – 50 – control points; c – 100 – control points

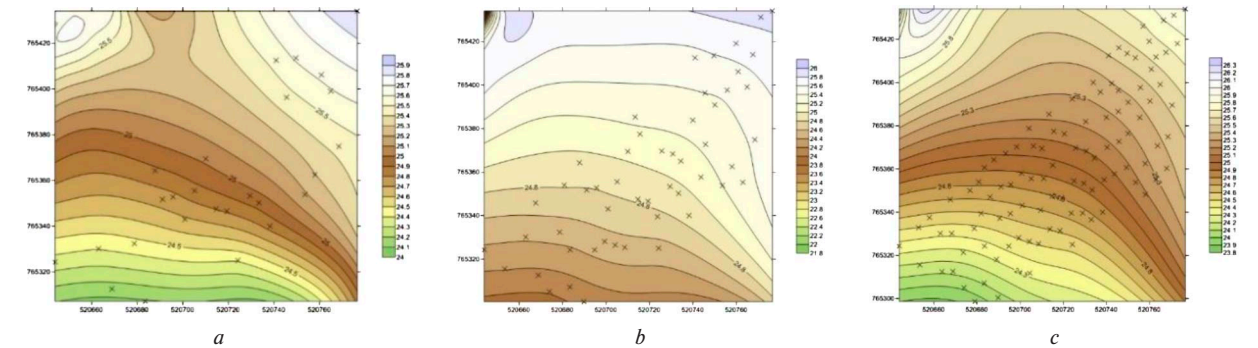

a *b* *c*

Fig. 7. Contour maps of geoid obtained from the Polynomial Regression Model (*Southern Zone*):
a – 25 – control points; b – 50 – control points; c – 100 – control points

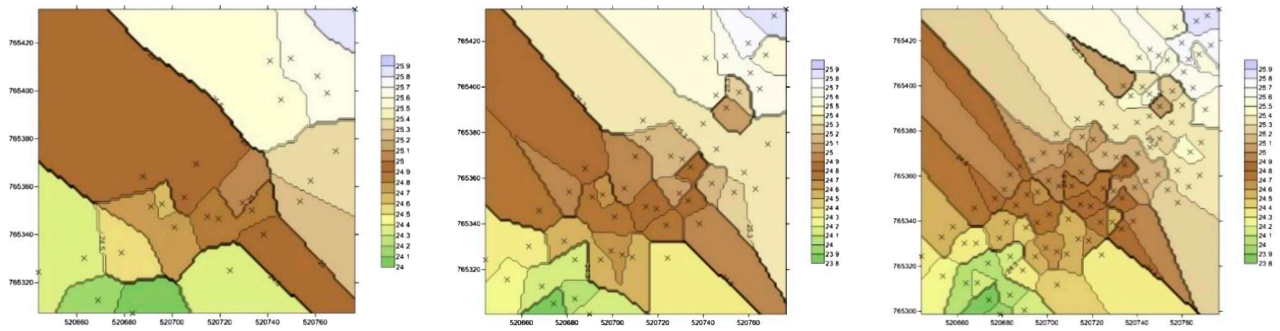

a *b* *c*

Fig. 8. Contour maps of geoid obtained from the Nearest Neighbour Model (Southern Zone):
a – 25 – control points; b – 50 – control points; c – 100 – control points

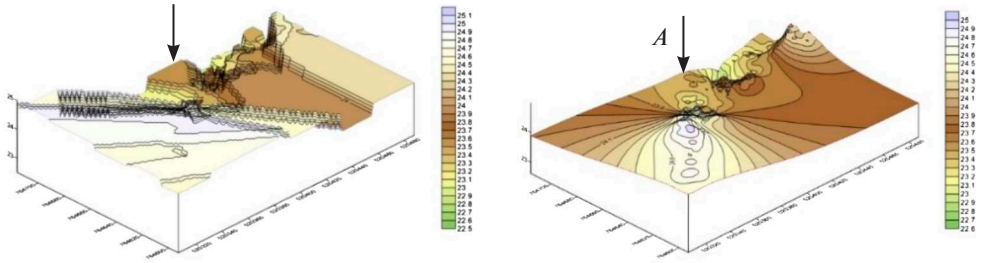

a *b*

Fig. 9. Contour maps with elevations of geoid obtained in Northern Zone:
a – from the Inverse Distance model; b – from the Nearest Neighbour Model

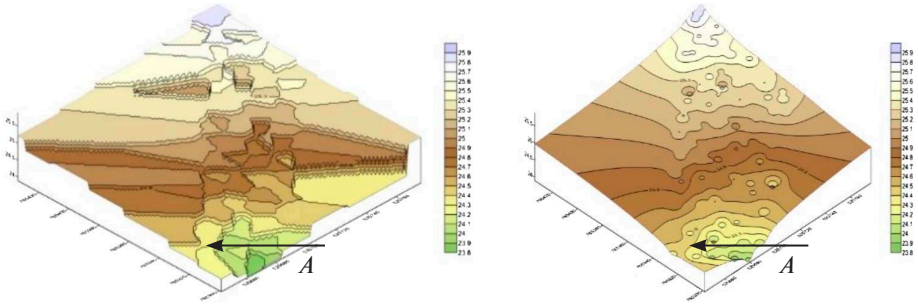

a *b*

Fig. 10. Contour maps with elevations of geoid obtained in Southern Zone:
a – from the Inverse Distance model; b – from the Nearest Neighbour Model

Conclusion. From the result obtained, the root mean square (RMS) values obtained from the control points of the southern zone are 0.31, 0.30, 0.27 and 0.27 for the geoid heights of all methods used, while 0.32, 0.31, 0.32 and 0.32 are obtained from the control points in the northern zone. These RMS values are very close in figure and it validates the geoid heights obtained from orthometric and ellipsoidal heights. In application it can be seen easily that RMS errors of this methods are very high. As a result of all evaluation polynomial regression, multi-quadratic and triangulation-interpolation methods can be used for geoid surface; these models equally promote enough accuracy for determination of orthometric heights from GPS alongside with Inverse distance and nearest neighbour models.

The most suitable geoid models for this quarry are the Inverse Distance and the Nearest Neighbour model. The deviation of these geoid models from GPS/levelling geoid model is ± 0.019 and ± 0.13 m at the northern and the southern zones. The value is smaller than root mean square values related to other global geoid models. It is thought that the cause of the situation is development of technology and better quality of data. When the distribution of differences in the quarry was examined, it was seen that there were bigger differences in the coast of the Polynomial Regression Model.

The elevation map obtained from different models heights, the sump location can be easily sited at the lowest elevation of the quarry face, with the overhead pressure, the rate of sipping of the ground water or the precipitation, the require pump power to discharge the water determined, the recommended pump machine can be acquired. Also the drilling of the blast-hole can be designed to give better aeration of water from the face to the sump.

Recommendations. The Mine Surveyors with Engineers should take note of the elevation diagrams and plan accordingly to promptly determine how the reserve is being depleted and also to construct accurate road network and precise sump sites that would not obstruct smooth flow of mining operations. Also the geological survey to increase the life of the deposit should continue.

Future research should look to application of geostatistical simulation in estimating the potential of the limestone reserve

as well as its variability. Moreover, the application of artificial intelligence i.e. neural networking should also be considered for estimation and prediction purposes of the reserve.

References.

1. Leavitt, B. R. (1999). Mine flooding and barrier pillar hydrology in the Pittsburgh basin. *Sixteenth annual international Pittsburgh Coal Conference*, *31*(36), 31042017. Retrieved from https://inis.iaea.org/search/search.aspx?orig_q=RN:31042017.

2. Reigber, C., Balmino, G., Schwintzer, P., Biancale, R., Bode, A., Lemoine, J.-M., & Zhu, S. Y. (2002). A high-quality global gravity field model from CHAMP GPS tracking data and accelerometry (EIGEN-1S). *Geophysical Research Letters*, *29*(14), 37.1-37.4. https://doi.org/10.1029/2002gl015064.

3. Abdalla, K. A. (2005). Unification of the Georeferencing Systems of GIS Spatial Data Infrastructure. *Proceedings of Map Middle East Conference*, 1-11. Retrieved from https://www.researchgate.net/publication/330500573.

4. Reigber, Ch., Jochmann, H., & Wunsch, J. (2004). Earth Gravity Field and Seasonal Variability from CHAMP. *Earth Observation with CHAMP*, 25-30. https://doi.org/10.1007/3-540-26800-6_4.

5. Skrypnyk, O., Shapar, A., & Taranenko, O. (2020). Determining local wetness conditions within the mined lands using GIS. *Mining of Mineral Deposits*, *14*(4), 53-58. https://doi.org/10.33271/mining14.04.053.

6. Kiamehr, R. (2001). Potential of the Iranian Geoid For GPS/Leveling. *Proc National Cartographic Center of Iran, Geomatics*, 1-10. Retrieved from https://www.academia.edu/714927.

7. Algarni, D. A. (1997). Geoid Modeling in Saudi Arabia. *ITC Journal*, (2), 114-120.

8. Reigber, C., Schwintzer, P., Neumayer, K.-H., Barthelmes, F., König, R., Förste, C., & Fayard, T. (2003). The CHAMP-only earth gravity field model EIGEN-2. *Advances in Space Research*, *31*(8), 1883-1888. https://doi.org/10.1016/s0273-1177(03)00162-5.

9. Akeju, V. O., & Afeni, T. B. (2015). Investigation of the spatial variability in Oyo-Iwa limestone deposit for quality control. *Journal of Engineering Science and Technology*, *10*(8), 1065-1085.

10. McClusky, S., Balassanian, S., Barka, A., Demir, C., Ergintav, S., Georgiev, I., & Veis, G. (2000). Global Positioning System constraints on plate kinematics and dynamics in the eastern Mediterranean and Caucasus. *Journal of Geophysical Research: Solid Earth*, *105*(3), 5695-5719. https://doi.org/10.1029/1999jb900351.

11. Watson, C. S., & Coleman, R. (1998). The Batman Bridge: structural monitoring using GPS. *Advances in GPS Deformation Monitoring*, 8. Retrieved from http://ecite.utas.edu.au/14264.

12. Çelebi, M., Prescott, W., Stein, R., Hudnut, K., Behr, J., & Wilson, S. (1999). GPS Monitoring of Dynamic Behavior of Long-Period Structures. *Earthquake Spectra*, *15*(1), 55-66. https://doi.org/10.1193/1.1586028.

13. Dvorak, J. J. (1992). Tracking the movement of Hawaiian volcanoes; Global Positioning System (GPS) measurement. *Earthquakes & Volcanoes (USGS)*, *23*(6), 255-267. Retrieved from https://pubs.usgs.gov/unnumbered/70039050/report.pdf.

14. Murray, M., Baxter, R., Karavas, B., & Burgmann, R. (1999). Permanent GPS network: Bay area regional deformation array. Annual Report, Berkeley CA, USA. Retrieved from https://seismo.berkeley.edu/annual_report/ar97_98/node7.html.

15. Kajzar, V. (2018). Geodetic and seismological observations applied for investigation of subsidence formation in the CSM mine. *Mining of Mineral Deposits*, *12*(2), 34-46. https://doi.org/10.15407/mining12.02.034.

16. Fotopoulos, G. (2005). Calibration of geoid error models via a combined adjustment of ellipsoidal, orthometric and gravimetric geoid height data. *Journal of Geodesy*, *79*(1-3), 111-123. https://doi.org/10.1007/s00190-005-0449-y.

17. Corchete, V., Chourak, M., & Khattach, D. (2005). The high-resolution gravimetric geoid of Iberia: IGG2005. *Geophysical Journal International*, *162*(3), 676-684. https://doi.org/10.1111/j.1365-246x.2005.02690.x.

Моделювання поверхні на основі визначення геоїда для боротьби з підтопленням у районі вапнякового родовища Евекоро (Нігерія)

А. П. Акінола[1], *Т. Б. Афені*[2], *Р. А. Осеменам*[2]

1 – Факультет гірничої промисловості, Університет Джоса, м. Джос, Нігерія, e-mail: akinolaa@unijos.edu.ng

2 – Факультет гірничої промисловості, Федеральний технічний університет Акуре, м. Акуре, Нігерія

Мета. Визначення висоти геоїда в різних контрольних точках кар'єра, розташованих у північній і південній зонах вапнякового родовища, що розробляє компанія Lafarge WAPCO Cement Ewekoro у штаті Огун, Нігерія.

Методика. Для визначення висот геоїда в різних контрольних точках кар'єра, розташованих у північній і південній зонах вапнякового родовища, були використані дані GPS і горизонтальної зйомки, що дозволили побудувати три моделі поверхні: поліноміальну модель регресії, модель інверсної відстані й модель найближчого сусіда. Дані моделі були використані для перехресної перевірки висоти геоїда в різних контрольних точках.

Результати. Результати дослідження показали, що розбіжність між значеннями висот геоїда, отриманими за допомогою GPS-горизонтальної зйомки та шляхом моделювання, знаходиться у межах 0,03 та 0,01 м відповідно. На основі моделей були складені контурні карти й позначені найкращі локації для відводу паводку.

Наукова новизна. Результати зіставлені з даними, що можна отримати у процесі експлуатації родовища.

Практична значимість. Підтоплення забою кар'єра можна краще регулювати, якщо створити дренажний відстійник у найнижчій точці карт висот і провести кероване буріння для забезпечення кращої аерації.

Ключові слова: *вапнякове родовище, GPS-горизонтальна зйомка, висота геоїда, моделі поверхні, боротьба з підтопленням*

Recommended for publication by Dr. Adeyemi Aladejare. The manuscript was submitted 27.02.21.